Supernovae

ismisebrendan

April 15, 2024

Abstract

The redshift of a number of type Ia supernovae (SNe Ia) and their host galaxies was determined from the redshift of a number of their spectral lines (most prominently the Hα line). The light curves of the same supernovae were analysed to find their peak B-band magnitudes and the luminosity-decline rate relation for each supernova. These peak magnitudes from the light curves were then standardised and used to plot a Hubble diagram along with the measured redshifts. The JLA SNe Ia sample was then used to plot a separate Hubble diagram and was compared to a number of cosmological models, a massless universe, a dark energy-less universe and the preferred model based on cosmic microwave background and SNe Ia measurements. It was found that in the whole dataset the massless model fit the best, but at redshifts above $z \sim 3 \times 10^{-2}$ the preferred model performed better, while the dark energy-less model was significantly diverged from the data at all times.

1 Introduction

Through the observation of Cepheid variable stars in a number of galaxies Hubble measured the distance to a number of galaxies and found that the distance to a galaxy, d, was directly proportional to its recessional velocity, v, according to

$$v = H_0 d \tag{1.1}$$

or, when the redshift, $z \ll 1$,

$$cz = H_0 d. \tag{1.2}$$

A plot which shows this known as a Hubble diagram and is conventionally plotted as distance against recessional velocity. [1]

Classical redshift is the apparent lengthening of the wavelength of light (reddening) as the source moves away from the observer. The redshift parameter, z, is defined as

$$z = \frac{\lambda_{obs} - \lambda_{em}}{\lambda_{em}} \tag{1.3}$$

where λ_{em} is the wavelength of the light in a reference frame at rest with respect to the source, and λ_{obs} is the observed wavelength of the light. [1]

Cosmological redshift is due to the stretching of light as the space between the source and observer expands. It is different from classical redshift, however the definition of z still holds. It also introduces cosmological time dilation, the relationship between the difference in time between when two events occurred, Δt_{em}, and the observed time difference, Δt_{obs}, and is given by

$$\frac{\Delta t_{obs}}{\Delta t_{em}} = 1 + z \implies \Delta t_{em} = \frac{\Delta t_{obs}}{1+z}. \text{ [1]} \tag{1.4}$$

The redshift of a galaxy (or any source) can be calculated by studying its spectra and the shift between the observed and (known) rest wavelengths of any spectral lines present.

Generally the distance modulus of a source, μ, the relation between its apparent and absolute magnitudes, m and M respectively, is given by

$$\mu = m - M = 5 \log_{10} (d[pc]) - 5. \text{ [1]} \tag{1.5}$$

Type Ia supernovae (SNe Ia) are the result of a C-O white dwarf in a binary (or greater multiple) star system increasing in mass beyond the Chandrasekhar limit (one measurement of which is $M_{Ch} = 1.38 M_\odot$ [2]) due to binary mass transfer. Due to their common progenitors SNe Ia are very homogeneous and so can be used a cosmological standardisable candles for distance measurement. [2], [3]

While they are not completely identical, they can be standardised. The difference in the peak magnitude of a SN Ia in the B-band and its magnitude after fifteen days, $\Delta m_{15}(B)$, were found to be related. This is known as the 'Phillips relation' or 'Luminosity-decline rate relation.' It was shown that the brighter SNe Ia in the B-band had slower declines in luminosity, i.e. lower values of $\Delta m_{15}(B)$. [3]

The luminosity-decline rate relation can be used to plot a Hubble diagram of the corrected apparent B-band magnitudes of supernovae against their redshift. The correction is given by

$$m_{B,corr} = m_B - \text{slope}\,(\Delta m_{15}(B) - 1.1) \qquad (1.6)$$

where m_B is the apparent magnitude of the SN Ia's peak, slope is the slope of the luminosity-decline rate relation and 1.1 simply corrects the observed magnitude of the SN Ia to the equivalent in the case of $\Delta m_{15}(B) = 1.1$ mag. [4]

A more modern method of correcting m_B has been developed over the last three decades. It relates the value of μ to m_B with a colour term c, approximately equivalent to the $B - V$ value at the maximum of the peak, and x_1, which is a measurement of the light curve shape, by

$$\mu = m^B - M_B + \alpha x_1 - \beta c \qquad (1.7)$$

where α and β respectively are coefficients for the light curve width and colour terms. M_B is the peak absolute magnitude of a SN Ia when $x_1 = c = 0$ and

- $\alpha = 0.141 \pm 0.006$,
- $\beta = 3.101 \pm 0.075$,
- $M_B = -19.05 \pm 0.02$ mag. [5], [6]

The value of M_B is adjusted in more massive galaxies to give

$$M_B = \begin{cases} M_B & \text{for } M_{stellar} < 10^{10} M_\odot \\ M_B + \Delta_m & \text{for } M_{stellar} \geq 10^{10} M_\odot \end{cases} \qquad (1.8)$$

where $\Delta_m = -0.07 \pm 0.02$ mag. [5]

The physical origin of this is uncertain, but its inclusion is due to the observed correlation between the peak luminosity of a SN Ia and the its host galaxy mass (and age, metallicity and star formation rate). [5]

2 Methods

2.1 Part A: measuring redshifts from spectra

The supernova spectral data was imported, and the flux values were normalised so that the highest flux value in each was equal to one. The list of typical spectral lines seen in galaxies was imported also, and the wavelengths of the different lines were stored.

The spectra, along with the Hα line, were plotted and it was determined that the galaxies all had a visible Hα line. This was fit to a Gaussian curve. The location of the peak of this Gaussian was used to find the redshift, z, of each galaxy using equation 1.3.

The spectra of the galaxies were then corrected for their respective redshifts and the spectra were plotted with all of the spectral lines superimposed. From this it was determined which lines were visible in which galactic spectra, then these lines (with the base, uncorrected wavelength data) were also fit to Gaussian curves to determine their redshifts. The mean of these values was taken to calculate the redshift of the respective galaxy.

In order to determine that each peak was fit correctly the data and the fit, as well as the guess at the fit were plotted. The initial parameters for the equation of the spectral line, which was taken to be a Gaussian curve of the form,

$$F(\lambda) = ae^{-\frac{(\lambda-b)^2}{2c^2}} + d, \qquad (2.1)$$

where, by default, $a = 0.5$, $c = 1$ and $d = 0.5$. While b was taken to be the location of the highest value of intensity in the data range unless otherwise specified.

2.2 Part B: measuring properties of the SN Ia light curves

The supernova light curve data was imported. The time data was adjusted so that the data all started from $t = 0$, simply to allow the fitting to work more easily. All of the times were corrected for time dilation according to equation 1.4. The B magnitude data was also checked to ensure that if there were values of 99.999 present they and the corresponding time and B magnitude uncertainty data were removed from the list, as these values occurred for times when no measurements were taken in the B band.

Polynomials of a number of degrees were fit to the one of the light curves in order to determine which was the most suitable for fitting the light curves. It was found that polynomials of degree 5, 6, and 7 gave good fits to the data for the area of interest, the peak time to 15 days after the peak.

A polynomial of each degree listed was fit to each light curve, and from this the peak of the light curve, $m_{max}(B)$, as well as the luminosity-decline rate relation were found. The means of these values obtained from each polynomial were taken for each light curve.

2.3 Part C: light-curve standardisation and the Hubble Diagram

The distance moduli, μ, for each galaxy were found using the preferred flat Λ cold dark matter model referenced in Part D of this assignment, with the Hubble parameter equal to $H_0 = 70$ km/s/Mpc and dark matter proportion, $\Omega_{m_0} = 0.3$. From this the absolute magnitudes of the peaks, $M_{max}(B)$ were found.

A plot was made of $M_{max}(B)$ against $\Delta m_{15}(B)$. A line was fit to this data by linear regression. The slope of this was taken and used to correct the B-band magnitude as in equation 1.6.

The apparent B-band magnitude was plotted against the base 10 logarithm of the redshift for both the corrected and uncorrected data. A linear fit was made against both of these datasets and the reduced χ^2 value for both fits was found and compared.

2.4 Part D

The supernova data was imported and the relevant data was split into separate variables. The distance modulus for each galaxy, μ was calculated according to equation 1.7.

For galaxies which were measured to have masses, $M_{stellar} < 10^{10} M_\odot$, but which had error bounds which included $10^{10} M_\odot$ (e.g. if the mass was measured to be $10^{9.4 \pm 0.7}$) the uncertainty in Δm was also included in the propagation of uncertainty of μ.

The distance moduli for the different models were calculated from the redshifts of the SNe. The models which were used were the two flat Λ, cold dark matter models discussed in the handout, the preferred model with $\Omega_M = 0.3$, and the model with no dark energy, i.e. $\Omega_M = 1.0$, as well as the model for a massless universe. In all cases the Hubble constant, H_0, was taken to be 70 km s^{-1} Mpc^{-1}. The distance, d, of a given redshift for the massless model is given by

$$d = \frac{cz}{H_0}\left(1 + \frac{z}{2}\right). \tag{2.2}$$

The distance modulus is then simply found by equation 1.5.

The different modelled distance moduli were plotted against the redshifts of the supernovae. The residuals were also plotted and the χ^2 value for each model was calculated, for the whole dataset as well as for selected subsets of the data.

Uncertainty was propagated in all instances and is detailed in Appendix A for the relevant sections.

3 Results

3.1 Part A: measuring redshifts from spectra

The spectra of SN1997bp and its host galaxy with the wavelength of the Hα line at rest marked is shown in figure 3.1.

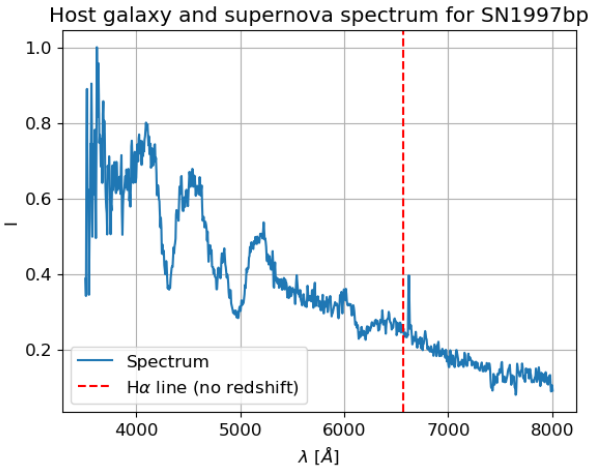

Figure 3.1: The spectrum of SN1997bp and its host galaxy with the wavelength of the Hα line marked.

A graphical example of the fitting of a Gaussian to the Hα peak is shown in figure 3.2, where the Hα line in the spectrum of SN1997E is being fit by a Gaussian curve.

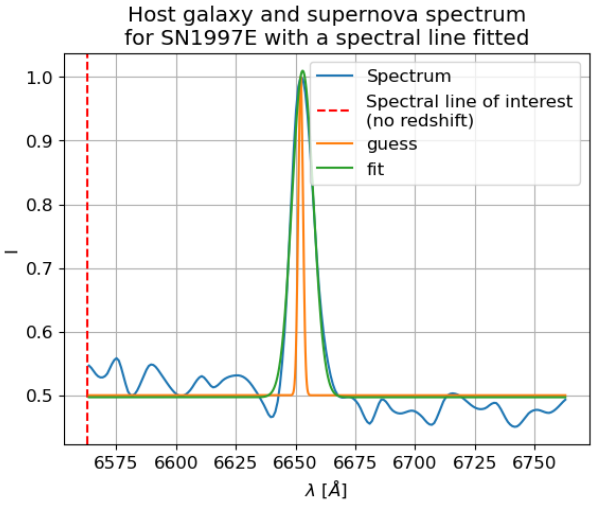

Figure 3.2: The Hα line in the spectrum of SN1997E being fit by a Gaussian curve with the initial guess at the fit also shown.

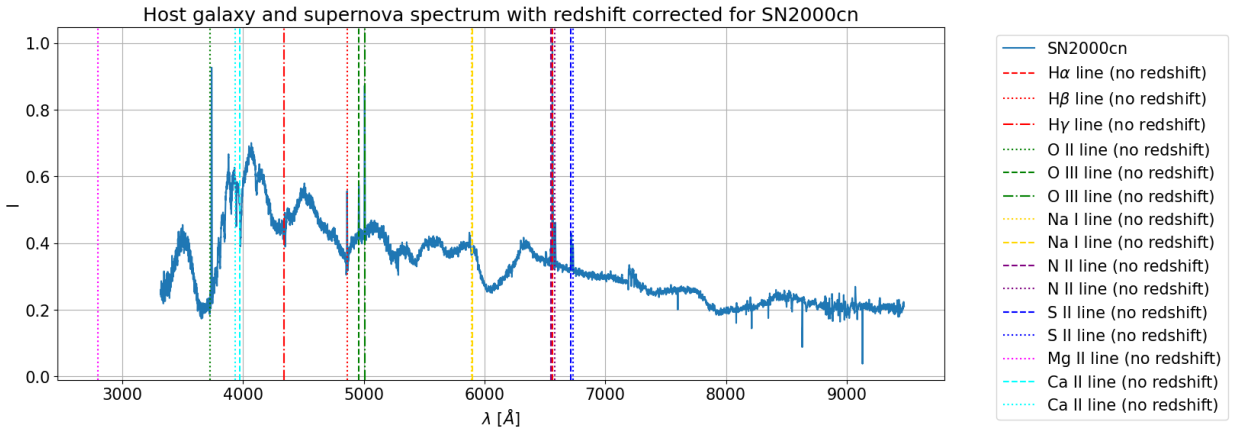

Figure 3.3: The corrected spectrum of SN2000cn and its host galaxy with the wavelength of a number of spectral lines marked. Note that a lot of them appear to line up well with peaks in the spectrum.

The spectrum of SN2000cn and its host galaxy with the wavelength corrected by the redshift calculated from fitting only the Hα line is shown in figure 3.3, notice how a number of the spectral lines appear to line up with a number of the peaks in the spectrum, this is the case for all of the spectra used in this lab.

The spectral lines used to find the redshift of each galaxy and supernova are listed below.

- SN1997bp: Hα, SI ($\lambda = 6717$ Å).
- SN1997E: Hα, Hβ, OII ($\lambda = 3727$ Å), OIII ($\lambda = 4959$ Å, $\lambda = 5007$ Å).
- SN1998es: Hα, OIII ($\lambda = 5007$ Å).
- SN1999aa: Hα, Hβ, OIII ($\lambda = 4959$ Å, $\lambda = 5007$ Å).
- SN1999dq: Hα, Hγ, NaI ($\lambda = 5890$ Å, $\lambda = 5896$ Å).
- SN2000cn: Hα, Hβ, Hγ, OII ($\lambda = 3727$ Å), OIII ($\lambda = 4959$ Å, $\lambda = 5007$ Å), NII ($\lambda = 6548$ Å, $\lambda = 6583$ Å), SII ($\lambda = 6717$ Å, $\lambda = 6731$ Å).
- SN2000dk: Hα, Hβ, NII ($\lambda = 6583$ Å).

As can be seen, the Hα line was visible in all spectra, however the amount and identities of the other lines that are visible for the other spectra varies widely.

The Gaussian curves were fit to all of the lines and the redshift, z, of each supernova averaged over all of the visible spectral lines is shown in table 3.1.

Table 3.1: The redshift z of each supernova, and therefore its host galaxy.

Supernova	z
SN1997bp	0.009(1)
SN1997E	0.0129(2)
SN1998es	0.0096(3)
SN1999aa	0.01301(13)
SN1999dq	0.0129(4)
SN2000cn	0.0236(2)
SN2000dk	0.0167(6)

For SN1999dq one of the CaII lines ($\lambda = 3969$ Å) was initially thought to line up and was fit, however this calculation gave a redshift of $z = 0.005(1)$ which is very different to the values of z calculated for the Hα, Hγ and two NaI lines of 0.014(1), 0.01157(11), 0.0122(0.0006) and 0.0138(0.0015) respectively. As such it was ignored in later calculations as it was unclear if that was the correct line.

Both CaII lines were also ignored in the calculations for SN2000cn for similar reasons.

3.2 Part B: measuring properties of the SN Ia light curves

Polynomials of degree 4, 5, 6 and 7 were fit to the light curve for each supernova, an example of this is shown for SN1999dq in figure 3.4.

It is clear that the fit is not very good for the polynomial of degree 4, for this light curve so it was not used in the following calculations. Also for all light curves and all polynomials the fit is not very good in the later parts of the light curve. However the only areas of interest are the peak in brightness

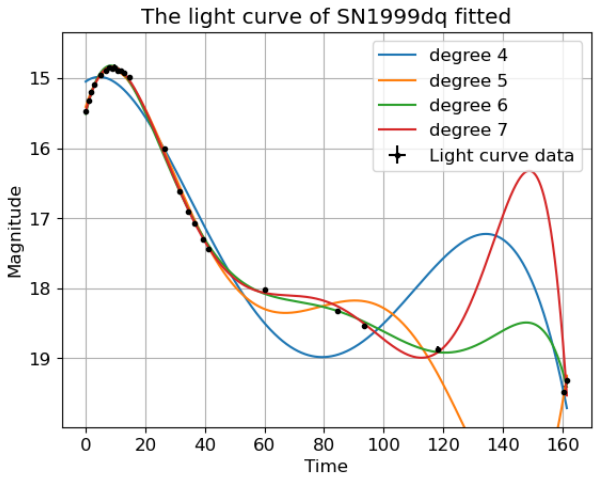

Figure 3.4: The light curve of SN1999dq and its host galaxy with polynomials of degree 4, 5, 6 and 7 fit to the data.

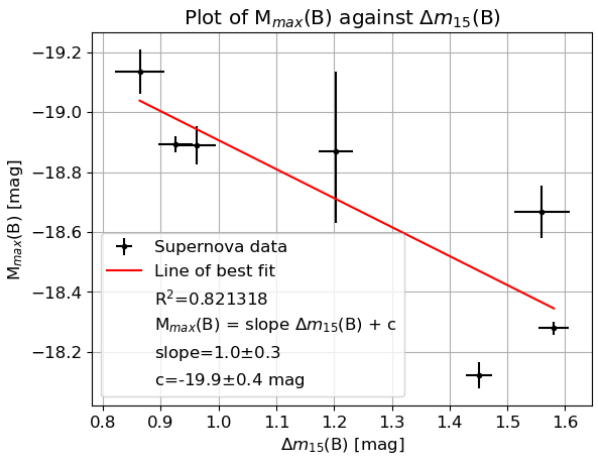

Figure 3.5: The absolute magnitudes of the SNe Ia plotted against the luminosity-decline rate relation with a line of best fit plotted.

and fifteen days after this, and in this light curve and all others the fit is very good for the region of interest for polynomials of degree 5, 6 and 7.

From the three fits which were made the average values of $m_{max}(B)$ and $\Delta m_{15}(B)$ were found and are listed in table

Table 3.2: The peak apparent B-band magnitude, $m_{max}(B)$, and luminosity-decline rate relation, $\Delta m_{15}(B)$, of each supernova.

Supernova	$m_{max}(B)$ [mag]	$\Delta m_{15}(B)$ [mag]
SN1997bp	14.087(9)	1.2(3)
SN1997E	15.614(1)	1.45(2)
SN1998es	13.96(2)	0.86(4)
SN1999aa	14.859(15)	0.93(3)
SN1999dq	14.842(18)	0.96(3)
SN2000cn	16.79(1)	1.58(3)
SN2000dk	15.63(18)	1.56(5)

3.3 Part C: light-curve standardisation and the Hubble Diagram

The distance moduli, μ, and therefore the absolute magnitudes in the B-band, $M_{max}(B)$, of each supernova was calculated and are shown in the plot in figure 3.5 against their luminosity-decline rate relation.

The apparent magnitudes were corrected and plotted against the redshift in a Hubble diagram as shown in figure 3.6.

As can be seen the reduced χ^2 value for the corrected magnitudes is much closer to 1 than it is for the uncorrected ones. This suggests that the correction to the peaks improves the use of SNe Ia as standardisable candles for distance measurements. The reduced χ^2 value is not very good however, and could likely be improved by including further measurements of supernovae.

3.4 Part D

The Hubble diagram for the SNe Ia is shown in figure 3.7.

The Hubble diagram for the different models and their residuals is shown in figure 3.8

The reduced χ^2 values were calculated for each of the models (note, these are not exactly the reduced χ^2 values as the χ^2 values were divided by the number of data points, not the number of data points less the number of fitting parameters, as I was unsure how many there were in the two flat Λ, cold dark matter models, so for simplicity and consistency the 'reduced χ^2 value' was taken as $\frac{\chi^2}{\text{no. data points}}$). They are shown on the plot for the entire dataset. As can be seen the reduced χ^2 value of the massless universe is closer to 1 than the preferred model is, suggesting that it is the correct model while the model without dark energy is relatively far from 1 so it can be concluded that this model is inaccurate.

If the differences between the reduced χ^2 values and 1 for the two models are plotted against the minimum redshift to be considered in the fitting of the two models the graph shown in figure 3.9 is obtained.

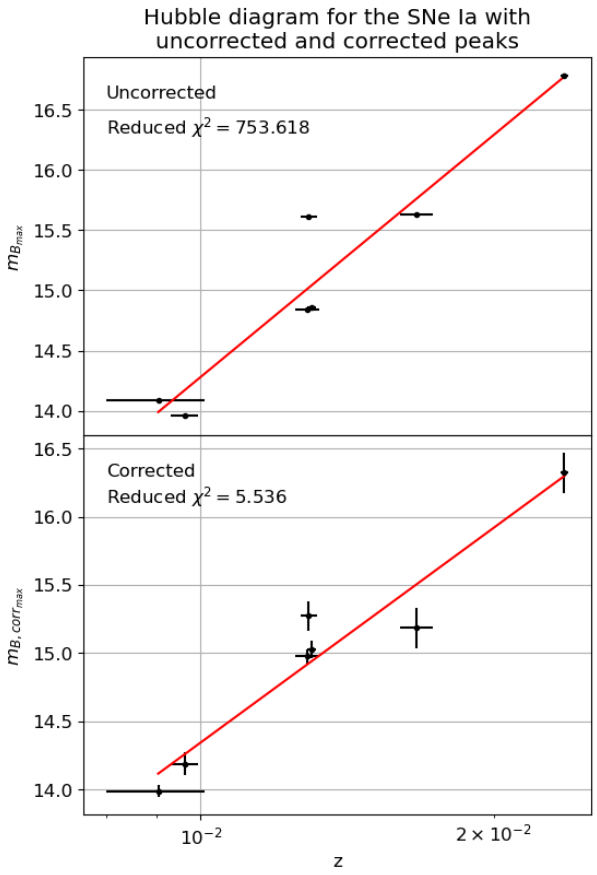

Figure 3.6: (Top panel) The Hubble diagram for these supernovae. (Bottom panel) The Hubble diagram for the same supernovae after the correction was made to the data.

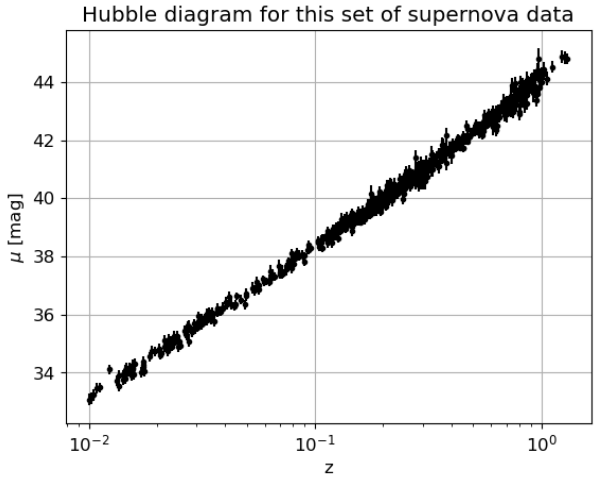

Figure 3.7: The Hubble diagram for the distance moduli of these supernovae.

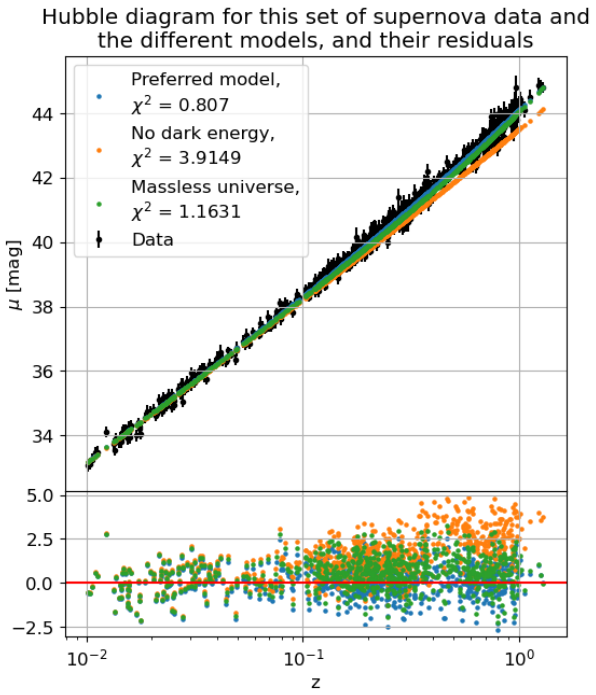

Figure 3.8: (Top panel) The Hubble diagram for the distance moduli of these supernovae for the data and the three different cosmological models used. (Bottom panel) The residuals of these models with respect to the data.

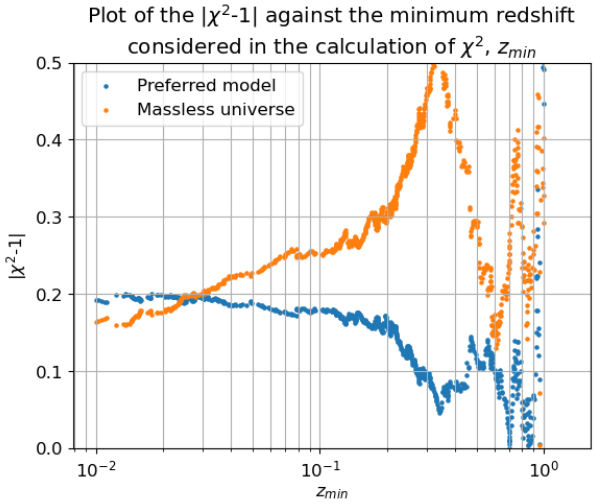

Figure 3.9: The value of $|\chi^2 - 1|$ against the minimum value of z considered in the calculation. Note that the large fluctuations in the values towards the right of the graph are likely due to the comparative lack of data points above this redshift value.

As seen in figure 3.9 the preferred model becomes a consistently better fit at redshifts above $z \sim 3 \times 10^{-2}$.

This suggests that there may be some local effects which influence (the measurement) of μ at small z.

4 Discussion and Conclusions

The combination of all of the measurements of the seven supernovae allowed for the plotting of a Hubble diagram, including the correction for the luminosity-decline rate relation as discussed in [4]. It produces a fit with a reduced χ^2 value of 5.536 which was significantly better than $\chi^2 = 753.618$ that was calculated for the uncorrected Hubble diagram. This is still very far from 1. However if perhaps some more supernovae were included in the measurements a better fit could perhaps be found. Alternatively, more accurate measurement of the redshifts, peak luminosities and luminosity-decline rate relations for the supernovae through better algorithms or, specifically for the calculation of the redshift, further observations of the spectra could also yield a better fit to the data.

The Hubble diagram was plotted for the JLA data and compared to various models. It was found that the model which ignores the existence of dark energy was the least accurate of the three models investigated. However, when the entire dataset is considered, the most accurate model was found to be that of a massless universe. When redshift values less than $z \sim 3 \times 10^{-2}$ are ignored it is found consistently that the preferred model is most accurate. This is likely due to some effects that affect either the measurement of μ at low z (or μ itself), or that there is less expansion than might be expected at these low redshifts.

A Propagation of Uncertainty

Here, I will be using δ to denote uncertainty in the interests of clarity as there are a number of terms elsewhere that use Δ to denote other values.

This makes use of Gauss's law of error propagation. If there is a function $f(x_1, x_2, ...)$ then the uncertainty in f, δf, is,

$$\delta f = \sqrt{\left(\frac{\partial f}{\partial x_1}\delta x_1\right)^2 + \left(\frac{\partial f}{\partial x_2}\delta x_2\right)^2 + ...} \qquad \text{(A.1)}$$

where δx_i is the uncertainty in x_i.

A.1 Part A: measuring redshifts from spectra

A.1.1 Uncertainty in redshift value

The uncertainty in the wavelength of the peak of a spectral line as determined by fitting a Gaussian curve to the peak in the supernova spectrum, $\delta\lambda$, was taken to be the full width half maximum of the peak. This is given by,

$$\delta\lambda = 2\sqrt{2\ln 2}\sigma \qquad \text{(A.2)}$$

where σ is the standard deviation of the peak.

The uncertainty in the redshift, δz, was found by propagating the uncertainty from $\delta\lambda$ as usual. Therefore

$$\delta z = \frac{\delta\lambda}{\lambda_0} \qquad \text{(A.3)}$$

where λ_0 is the wavelength of the spectral line in an at-rest reference frame.

When calculating the average value of z for all relevant spectral lines in the combined galaxy, supernova spectra the calculated values of $z \pm \delta z$ were also included. This does not affect the average value obtained, but it does affect the standard deviation and incorporates the uncertainty in the individual values into the calculation of the standard deviation. This standard deviation was then taken as the uncertainty in the mean value of z for the supernova.

A.2 Part B: measuring properties of the SN Ia light curves

A.2.1 Uncertainty in corrected time

The time data provided in this part t_{obs} was corrected for time dilation to give the time data used, t_{em}, by equation 1.4

The uncertainty in t_{em} was then calculated by

$$\delta t_{em} = \sqrt{\left(-\frac{t_{obs}}{(1+z)^2}\delta z\right)^2} = \left|-\frac{t_{obs}}{(1+z)^2}\delta z\right| \qquad \text{(A.4)}$$

A.2.2 Uncertainty in peak value and decline rate

The value of the peak is given by the local minimum of a polynomial describing the B-band magnitude against time, $B(t_{em})$, of degree n where $n = 5, 6, 7$, with coefficients $c_0, c_1, ...c_n$, each having an associated uncertainty, $\delta c_0, \delta c_1, ...\delta c_n$. The polynomial has the form

$$B(t_{em}) = \sum_{r=0}^{n} c_r \left(t_{em}\right)^{n-r}. \tag{A.5}$$

The uncertainty in B for a given value of t_{em}, $\delta B(t_{em})$ is given by

$$\delta B(t_{em}) = \sqrt{\sum_{r=0}^{n} \left(\delta c_r\right)^2 \left(t_{em}\right)^{n-r}}. \tag{A.6}$$

This was used to find the uncertainty in the value of the peak and in the value of the decline rate, $\delta(\Delta m_{15}(B))$, by finding the value of $\delta B(t_{em})$ for different values of t_{em}.

When finding the mean values of the peak and decline rate for all polynomials the same strategy as was employed in the determination of the redshift of including the value $\pm$ the uncertainty in the calculation of the mean and standard deviation was used. Again, the standard deviation of these samples was taken as the uncertainty in the values.

A.3 Part C: light-curve standardisation and the Hubble Diagram

A.3.1 Uncertainty in distance modulus

The upper and lower uncertainties in the distance moduli were found by finding the distance moduli for the redshift values with the uncertainties added to/subtracted from them, and then finding the difference between them and the actual values of μ. These errors were then propagated as normal, the absolute magnitude of the peak, $M_{max}(B)$, is given by

$$M_{max}(B) = m_{B_{max}} - \mu \tag{A.7}$$

where $m_{B_{max}}$ is the apparent magnitude of the peak, meaning the uncertainty in $M_{max}(B)$ is given by

$$\delta M_{max}(B) = \sqrt{\left(\delta m_{B_{max}}\right)^2 + \delta\mu^2}. \tag{A.8}$$

A.3.2 Uncertainty in corrected magnitude

The corrected magnitude is given by equation 1.6, meaning the uncertainty in the corrected magnitude, $\delta m_{B,corr_{max}}$ is given by

$$\begin{aligned}\delta m_{B,corr_{max}} = \Big(&(\delta m_{Bmax})^2 \\ &+ \left(\Delta m_{15}(B) - 1.1\right)^2 \left(\delta\text{slope}\right)^2 \\ &+\text{slope}^2 \left(\delta\Delta m_{15}(B)\right)^2\Big)^{1/2}.\end{aligned} \tag{A.9}$$

A.4 Part D

A.4.1 Uncertainty in distance modulus

The distance modulus is given by 1.7, therefore the uncertainty in its value, $\delta\mu$ is

$$\begin{aligned}\delta\mu = \Big(&\left(\delta m_*^B\right)^2 + \left(\delta M_B\right)^2 + x_1^2\delta\alpha^2 \\ &+\alpha^2 \left(\delta x_1\right)^2 + c^2\delta\beta^2 + \beta^2\delta c^2\Big)^{1/2}\end{aligned} \tag{A.10}$$

where, due to the definition of M_B in equation 1.8,

$$\delta M_B = \begin{cases} \delta M_B & \text{for } M_{stellar} < 10^{10} M_\odot \\ \sqrt{\left(\delta M_B\right)^2 + \left(\delta\Delta_m\right)^2} & \text{for } M_{stellar} \geq 10^{10} M_\odot \end{cases}. \tag{A.11}$$

References

[1] B. W. Carroll and D. A. Ostlie, *An Introduction to Modern Astrophysics*, 2nd ed. Cambridge University Press, 2017.

[2] P. A. Mazzali, F. K. Röpke, S. Benetti, and W. Hillebrandt, "A common explosion mechanism for type ia supernovae," *Science*, vol. 315, no. 5813, pp. 825–828, 2007. [Online]. Available: https://www.science.org/doi/abs/10.1126/science.1136259

[3] M. M. Phillips, "The Absolute Magnitudes of Type IA Supernovae," ApJ, vol. 413, p. L105, Aug. 1993.

[4] M. Hamuy, M. M. Phillips, J. Maza, N. B. Suntzeff, R. A. Schommer, and R. Aviles, "A Hubble Diagram of Distant Type 1a Supernovae," AJ, vol. 109, p. 1, Jan. 1995.

[5] D. M. Scolnic *et al.*, "The Complete Light-curve Sample of Spectroscopically Confirmed SNe Ia from Pan-STARRS1 and Cosmological Constraints from the Combined Pantheon Sample," ApJ, vol. 859, no. 2, p. 101, Jun. 2018.

[6] R. Tripp, "A two-parameter luminosity correction for Type IA supernovae," A&A, vol. 331, pp. 815–820, Mar. 1998.